IOP Publishing Semiconductor Science and Technology
Semicond. Sci. Technol. **36** (2021) 045028 (7pp) https://doi.org/10.1088/1361-6641/abe24e

Defect states and passivation mechanism at grain boundaries of zinc-blende semiconductors

Hong-Yang Gu[1,2], Wan-Jian Yin[3,4] and Xin-Gao Gong[1,2]

[1] Key Laboratory for Computational Physical Sciences (MOE), State Key Laboratory of Surface Physics, Department of Physics, Fudan University, Shanghai 200433, People's Republic of China
[2] Collaborative Innovation Center of Advanced Microstructures, Nanjing 210093, People's Republic of China
[3] College of Energy, Soochow Institute for Energy and Materials InnovationS (SIEMIS), and Jiangsu Provincial Key Laboratory for Advanced Carbon Materials and Wearable Energy Technologies, Soochow University, Suzhou 215006, People's Republic of China
[4] Key Lab of Advanced Optical Manufacturing Technologies of Jiangsu Province and Key Lab of Modern Optical Technologies of Education Ministry of China, Soochow University, Suzhou 215006, People's Republic of China

E-mail: xggong@fudan.edu.cn

Received 8 September 2020, revised 23 January 2021
Accepted for publication 2 February 2021
Published 25 March 2021

Abstract

Grain boundaries (GBs) are significant in determining the electrical properties of polycrystalline semiconductors. However, the electronic structures and passivation mechanisms of polycrystalline semiconductors remain poorly understood. In this study, we systematically investigated the Σ3 (112) GB properties of several typical zinc-blende semiconductors via first-principles density functional calculations. We found significant differences of Σ3 (112) GB structures and properties between IV/III and V types, where dangling atoms formed new covalent bonds, and II–VI/I–VII types, where dangling atoms formed no new bonds. These different bonding configurations lead to different origins of defect states at GBs. We successfully designed a targeted doping approach to passivate such defect states for different types of semiconductors. We demonstrated the validity of the proposed approach in Σ3 (112) GB of the zinc-blende semiconductors. This work elucidates the defect states at GBs in common zinc-blende semiconductors, rationalizes diverse post-treatment approaches reported in previous experiments, and provides general guidance for defect passivation at the GBs of polycrystalline semiconductors.

Keywords: grain boundary, passivation mechanism, zinc-blende semiconductor

(Some figures may appear in colour only in the online journal)

1. Introduction

Grain boundaries (GBs) are important in determining the mechanical, optical, and electronic properties of polycrystalline materials [1–7]. The study and engineering of GBs have attracted significant scientific interest for many decades. In polycrystalline solar-cell absorbers, GBs can significantly influence the photoelectric properties by creating large amounts of deep defect levels and providing effective carrier recombination pathways [8–10]. Therefore, GBs are among the key factors affecting the performance of solar cells. Fully understanding the electronic structures of GB is necessary to provide passivation mechanisms for defect states and thus enhance the power conversion efficiencies (PCEs) of solar cells.

Despite having similar crystal structures, the approaches for defect passivation at GBs differ among different zinc-blende compounds. The II–VI semiconductor CdTe and its

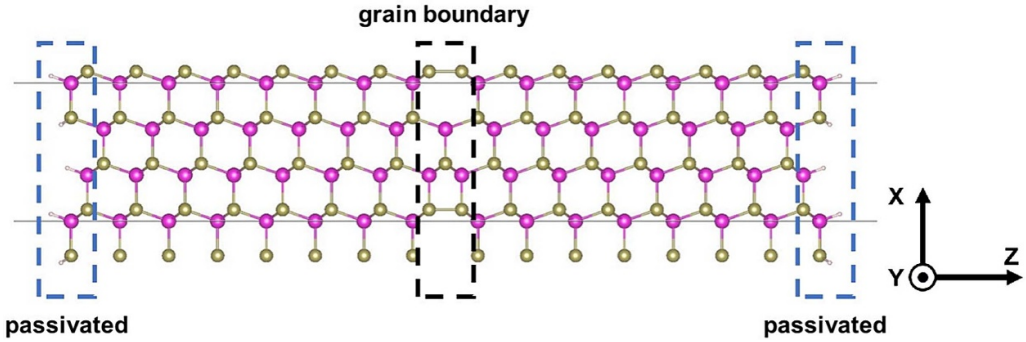

Figure 1. The structure model of GB used in the simulation. The *X* and *Y* directions of the simulation cell are periodic, while the cell along *Z* direction is finite passivated by pseudohydrogens.

derivative Cu(In,Ga)Se_2 can reach high PCEs with the existence of high-density GBs, because post-treatments effectively heal the defect levels at GBs [11, 12]. Recently these processes were theoretically understood by the concise concept of the self-passivation mechanism [13], i.e. the defect level of GBs in these semiconductors can be passivated by appropriate cations. For example, Cd and Na can passivate the defect levels in CdTe and $CuInSe_2$/Cu_2ZnSnS_4 GBs, respectively [13, 14]. In contrast, for Si and GaAs, self-passivation is ineffective and post-treatments designed for GB passivation with external impurities are required [15, 16]; this partially explains the difficulties of defect passivation in Si or III–V compounds relative to that in II–VI compounds. Instead, special passivation procedures are necessary for solar cells based on Si and III–V compounds. For example, the selective anodization technique is useful in GaAs [17–19], and hydrogen doping can suppress the harmful effects of GBs in Si semiconductors [15, 20–22]. Notably, all these semiconductors have the same zinc-blende structures; the atomic structures of the corresponding GBs are also similar [23–25], but the defect properties are obviously different. The fundamental physics underlying this striking difference has never been understood.

In this research, we systematically study the electronic structures of GBs from different groups, including I–VII, II–VI, III–V, and IV semiconductors, by using first-principles calculations. We find that the electronic properties of I–VII and II–VI semiconductor GBs are intrinsically different from those of III–V and IV semiconductor GBs. We identify the distinct bonding configurations at GBs as the source of this difference. The dangling atoms at GBs in IV and III–V types tend to form covalent bonds, while those in II–VI and I–VII do not. This difference in bonding character leads to different passivating mechanisms. These mechanisms can be understood according to a straightforward approach of electron counting at the atoms in a GB that contribute gap states. Based on these, we arrived at a general passivation rule and for the first time proposed that defect levels in GaAs GB can be easily passivated by proper doping.

2. Computational methods

The density functional calculations were performed by using VASP code [26]. We used projector-augmented wave [27] with the local density approximation to do the simulations [28]. The cutoff energy for the plane-wave basis was 400 eV and the energy convergence parameter was set to be 10^{-4} eV. The structural optimization was terminated until the Hellmann–Feynman forces less than 0.02 eV $Å^{-1}$.

We chose the widely existing symmetric Σ3 (112) GB as our GB calculation model, whose structure has been confirmed in experiments [23–25]. To avoid the possible internal electric field interaction, we employed only single GB in the simulation slab with about 20 Å vacuum layers to separate the slab, as illustrated in figure 1. Each simulation slab contained 47 anions and 47 cations and the *k*-points were sampled with $15 \times 15 \times 1$ mesh in the Brillouin zone. As for calculations related to the self-passivation rule, we used the $1 \times 2 \times 1$ supercells (with 94 anions and 94 cations) of the prototype GB slabs and the *k*-points were sampled with $15 \times 7 \times 1$. In order to eliminate the influence from the surface dangling bonds [29, 30], pseudo-hydrogens were used to passivate the surface states. The formation energies were calculated by the formula $E_f = E_{tot} - \sum^{n_i} \mu_i$, where n_i and μ_i were the number and chemical potential of the corresponding atom. For each semiconductor, sum of the two element potential should be equal to the total energy of the bulk semiconductor and each chemical potential is supposed to be lower than that of the elementary substance. In this paper, for all the 12 considered semiconductor Σ3 (112) GBs, all the anion-core GBs have lower formation energy than the corresponding cation-core GBs. So we only focus on the properties of the more stable GB structures.

3. Results and discussion

3.1. Bonding configuration of dangling atoms at GBs

We studied the anion core Σ3 (112) GB for group IV, III–V, II–VI, and I–VII semiconductor types, with each group represented by the three compounds, which belongs to zinc-blende structures or diamond structures, with the calculated properties listed in table 1. We find that semiconductors with different types differ significantly in their structural relaxations at GBs. However, the anion-core distance of the same type show almost the identical deformation trends (table 1). To quantify the atomic relaxation at GBs, we define the bond length difference as the change in bond length relative to the bond length

Table 1. The calculated structure and properties of anion core grain-boundary in zinc-blende semiconductors. The bond difference is defined as the bond length changes related to the bond length in the bulk. The relative energy is the difference of the formation energy between the reconstructed structure with the complex defect (a cation vacancy plus a cation interstitial) and the prototype GB. The GBs from various groups show significant different behavior, while those from the same group are similar to the other.

	Group	Bond difference	Relative energy (eV)
AgBr	I–VII	41.3%	−0.83
CuBr	I–VII	34.6%	−0.44
CuCl	I–VII	51.8%	−0.49
CdTe	II–VI	22.6%	−0.17
ZnSe	II–VI	26.5%	−0.06
ZnTe	II–VI	21.1%	−0.02
GaAs	III–V	−2.8%	0.87
InSb	III–V	−3.4%	0.38
InP	III–V	−0.9%	Not stable
Si	IV	0.6%	Not stable
Ge	IV	1.1%	Not stable
SiC	IV	3.4%	Not stable

in the bulk system. For group IV semiconductors, the bond lengths are almost unchanged, and for the III–V semiconductors, they are only slightly reduced. In contrast, for the II–VI, the bond length is increased by >20% at the GB core; the degree of increase is even larger for I–VII semiconductors. These significant differences in atomic structure suggest that these GBs may have different electronic properties.

To distinguish the electronic structures, the charge density differences are shown in figure 2. For group IV and III–V semiconductors, such as Si and GaAs, new covalent bonds are formed in the GB (see the arrows in the figure) without significant bond relaxation. However, for the group I–VII and II–VI semiconductors, such as AgBr and CdTe, significant structural relaxation increases the inter-atomic distance and prevents bond formation in the GB core. We find that, as discussed below, such a re-organization of charge density in the GB core can be closely related to the appearance of gap states.

The different bonding configuration at GB core can be qualitatively understood by bond covalency of semiconductor, following the sequence, IV (typical covalent) >III–V > II–VI > I–VII (typical ionic). In covalent systems, the dangling atoms tend to form covalent bond by sharing the non-bonding electron with the nearby atoms to lower the electronic energy. While in ionic systems, the electronic shells of dangling atoms are saturated, therefore, there is no energetical tendency to form covalent bonds.

3.2. Origin of defect levels at GBs

It was previously shown that defect states in the band gap are mostly induced by dangling bonds or wrong bonds of atoms at GB cores [3, 31, 32]. The calculated local electronic density of states (LDOS) for each of the atoms at the GB cores are shown in the lower panel of figure 2. In an I–VII semiconductor such as AgBr, no defect states exist in the gap. For a II–VI semiconductor such as CdTe, the defect level states are mostly contributed by two Te atoms at the GB core, which is consistent with previous studies [4, 33, 34]. The extra Cd–Te bond at the bottom of the seven-membered ring does not contribute much to the gap states.

For the group IV and III–V semiconductors such as Si and GaAs, the gap states are not derived from the anion cores because of the formation of new covalent bonds. The LDOS of the As-core atom is not inside the band gap, while ∼0.6 eV above the Fermi energy. On the contrary, the Ga1/Ga2 atoms near the As core contribute most of the defect states, even though they have no wrong bonds or dangling bonds. For a Si GB, the Si1/Si2 atoms at the identical anion-core site also introduce no defect levels in the band gap.

For greater clarity, the charge density of the selected defect level is plotted as shown in figure 3. For CdTe, the defect state shown in figures 3(a) and (b) is a dangling bond state; the distance between two Te atoms is large and no bond is formed. Unlike the Te dangling bonds at the CdTe GB core, two As atoms form a covalent bond in the GaAs GB core. The new bonding state formed between two As atoms in the GaAs GB core is pushed down far below the valence band maximum (VBM) (figure 3(g)), while its anti-bonding state is pushed up to exceed the VBM. The defect levels of the GaAs GB shown in figure 3(e) are mainly from the atoms near the bottom of the seven-membered ring.

3.3. Reconstructions for II-VI and I-VIII GBs

The different electronic origins of the gap states in II–VI and III–V/IV semiconductors are responsible for their different passivation mechanisms. For the II–VI semiconductor, the defect states are derived from the dangling atoms at the GB interface. In this sense, the defect states can be passivated by forming a complex defect (a cation vacancy plus a cation interstitial) or directly doping with their own cations at the GB interface in the II–VI semiconductor. Such doping or forming the complex defect can also be kinetically favorable because GB interfaces are considered channels for ion diffusion, thus facilitating defect passivation. This is why the self-passivation rule and post-treatment is useful and important for chalcogenide semiconductors [13, 14]. We further confirmed the applicability to passivate defect states of the both two reconstructions in other II–VI semiconductors, such as ZnTe and ZnSe. For the I–VII type, although no clear defect state exists in the gap, the formation of a complex defect, such as $Ag_i + V_{Ag}$ in an AgBr GB, can increase the GB stability without generating deep levels. As listed in table 1, we confirmed that the same reconstruction of breaking the mirror symmetry at boundary in II–VI also works in I–VI semiconductors.

In contrast, this symmetry broken construction can neither passivate the defect states nor enhance the stability of the III–V and IV semiconductor GBs. For example, the defect configuration of $Ga_i + V_{Ga}$ at the GaAs GB increases the formation energy by 0.87 eV and introduces a new deep level. For Si, the complex defect configuration is unstable. This is consistent with a previous study using the self-passivation rule to investigate the passivation mechanism of InAs GB [35]. They

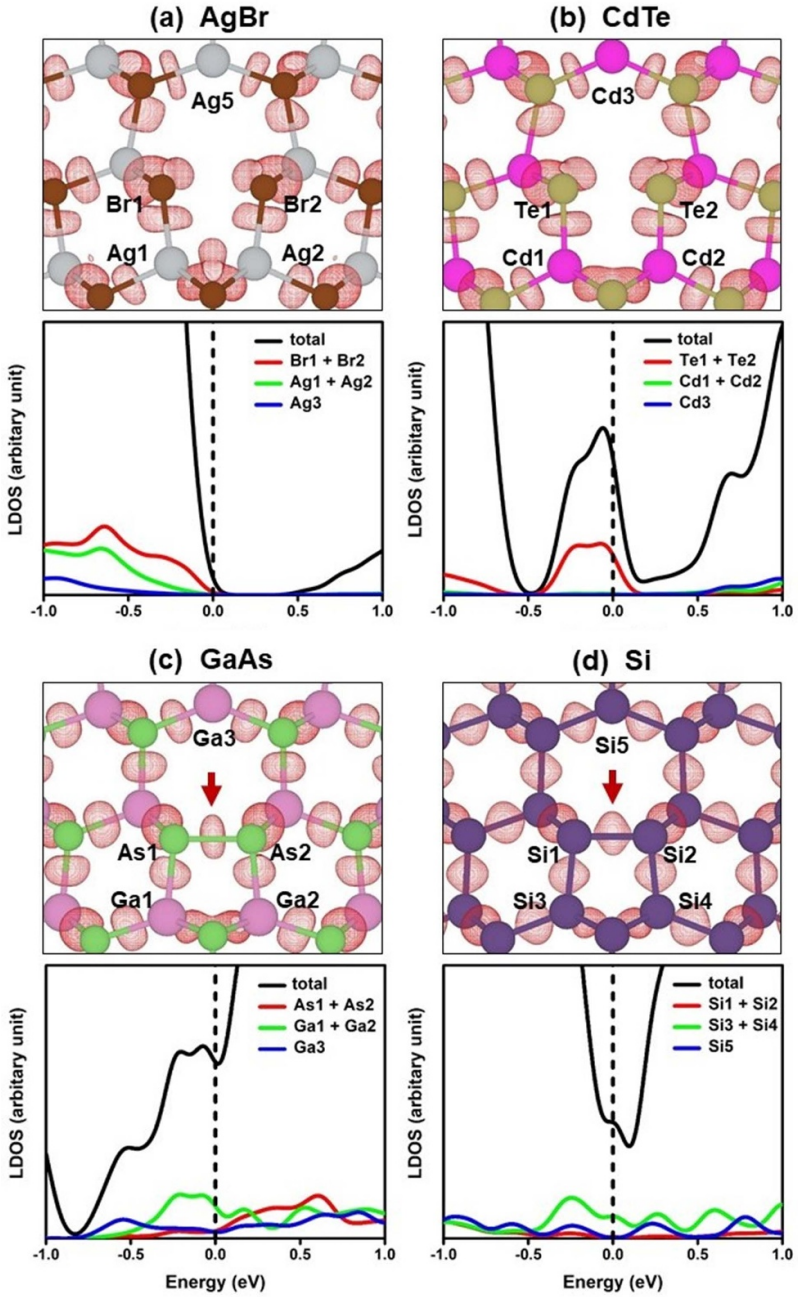

Figure 2. The charge density difference and local density of states (LDOS) for Σ3 (112) anion-core GBs of AgBr, CdTe, GaAs and Si. The arrows in (c) and (d) indicate the covalent charge accumulated between two atoms where there are no direct bonds in the bulk. The vertical dashed lines represent the Fermi energy. The formation of new bonds leads to the source of the deep levels changed.

reported that $In_i + V_{In}$ GB yielded imperfect passivation of the anion wrong bond, and that doping with In atom or other elements could not open the band gap either. Results for other III–V and IV group semiconductors are summarized in table 1. In these semiconductors, the valence shells of anion-core atoms are fully occupied with the aid of shared electron pairs at the newly formed covalent bond. The anion-core does not contribute to the gap state. The added doping cation does not have a corresponding dangling bond. Mandatory changes in the stable covalent bonds introduce additional strain energy to the system and yield a structure with more harmful electronic structures. As a result, the complex defect configurations of III–V and IV semiconductors are not the stable and passivated structures because of the covalent bonds formed at the GB core.

3.4. Electron counting and passivation mechanism

In order to determine a possible passivation mechanism for III–V semiconductor GBs, we adopt a straightforward approach of electron counting at GB atoms that contribute to gap states. The gap states and charge density plots are shown in figure 3, where GaAs and CdTe are taken as examples for III–V and II–VI semiconductors, respectively. The details of

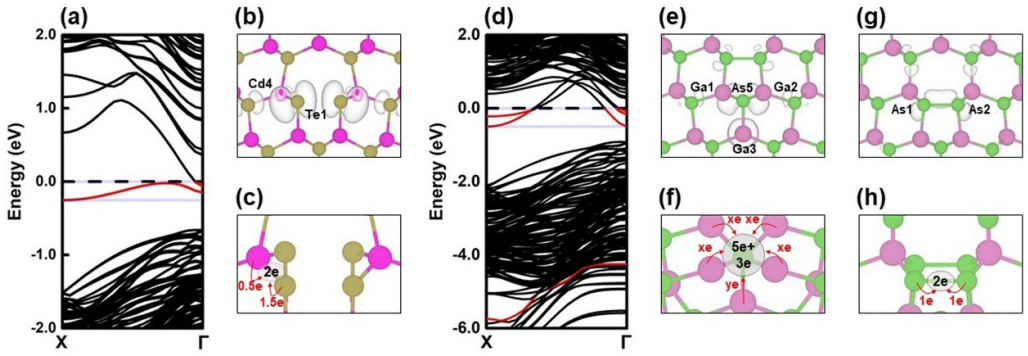

Figure 3. The band structure and charge density for the selected states (labeled in red). (a), (b) CdTe, (d), (e) and (g) for GaAs GBs. (b), (e) denote the summed charge densities of corresponding defect states at all the *k*-points. (g) is the calculated charge density at Γ point for the state labeled in red below the GaAs VBM. (c), (f) and (h) are electron transfer diagrams for corresponding GBs. Only the abnormal bonds are labeled in the diagrams, other covalent bonds can be regarded as normal bonds. The CdTe GB presents a dangling bond state under the Fermi energy (the dash line) as the deep levels. The anti-bonding and bonding state in GaAs are not the main source of the deep levels.

Table 2. Electron counting computation of GaAs and CdTe GB. The atoms listed in the table are those defect states mainly come from as labeled in figure 3. The number of electrons transferred from Ga1/Ga2 to nearby single abnormal bond is supposed to be x, and y for Ga3. The abnormal bonds include the wrong bonds and the bonds whose bond length alters much. Note that $4x + y = 3$, according to octet occupation of As5. The redundant electrons for GaAs and CdTe GBs are 2 e and 3 e, respectively.

GB type/Atom	Valence electron	Normal bond	Abnormal bond	Extra electron
(a) GaAs Σ3 (112) As-core				
As1	5	3 × 1.25	1 × 1	0.25
As2	5	3 × 1.25	1 × 1	0.25
Ga1	3	2 × 0.75	2 × x	1.5–2 × x
Ga2	3	2 × 0.75	2 × x	1.5–2 × x
Ga3	3	2 × 0.75	1 × y	1.5–1 × y
Total				5–4x—$y \rightarrow 2$
(b) CdTe Σ3 (112) Te-core				
Te1	6	3 × 1.5	0	1.5
Te2	6	3 × 1.5	0	1.5
Total				3

electron counting are summarized in table 2. The conclusions can be extended to other semiconductors of the same type.

In the zinc-blende GaAs bulk system, each As(Ga) atom forms covalent bonds with the four nearest Ga(As) atoms, respectively. Based on the octet electron rule, 1.25 e from each As atom and 0.75 e from each Ga atom make up each covalent bond. As shown in figure 3, abnormal bonds mainly originate from two regions, around the As1/As2 anion core (figure 3(h)) and the As5 atom (figure 3(f)). All the As–Ga wrong bonds are related to the As5 atom, while the other As–Ga bonds are similar to those in the bulk. In the first region, the As1 and As2 form a covalent wrong bond with a pair of shared electrons (figure 3(h)), while the other three are normal As–Ga bonds. The total number of electrons from As1/As2 participating in the bond is $2 \times (1.25 \times 3 + 1 \times 1) = 9.5$. Therefore, there are $2 \times 5(\text{As}) - 9.5 = 0.5$ excess electrons in the first region associated with the As1/As2 atoms, because each As atom has five valence electrons. As for the second region, the defect states mainly arise from the Ga1/Ga2 and Ga3 atoms. Ga1 and Ga2 atoms form four normal As–Ga bonds and four As–Ga abnormal bonds. If x is the number of electrons transferred from the Ga atom to the Ga1/Ga2–As5 bond, the total number of electrons from Ga1 and Ga2 participating in bonding is $4 \times 0.75 + 4x$. The Ga3 atom has two normal As–Ga bonds and one Ga3–As5 abnormal bond. If y is the number of electrons transferred to the Ga3–As5 bond from Ga3, then the number of electrons from Ga3 participating in bonding is $2 \times 0.75 + y$. Because there are almost no defect states associated with the As5 atom, it should reach octet saturation (figure 3(f)), so the number of valence electrons from Ga atoms forming bonds should be 3, i.e. $4x + y = 3$. The number of redundant electrons in the second region associated with the As5 atom is the sum of the valence electrons from Ga1/Ga2 and Ga3 minus those involved in bond formation: $[6 - (4 \times 0.75 + 4x)] + [3 - (2 \times 0.75 + y)] = 1.5$. The computation procedure is shown in table 2. The total number of excess electrons in the whole GB is $1.5 + 0.5 = 2$, indicating that the defect states in the GB are equivalent to two doped electrons. This is consistent with the DOS calculation (figure 3(d)).

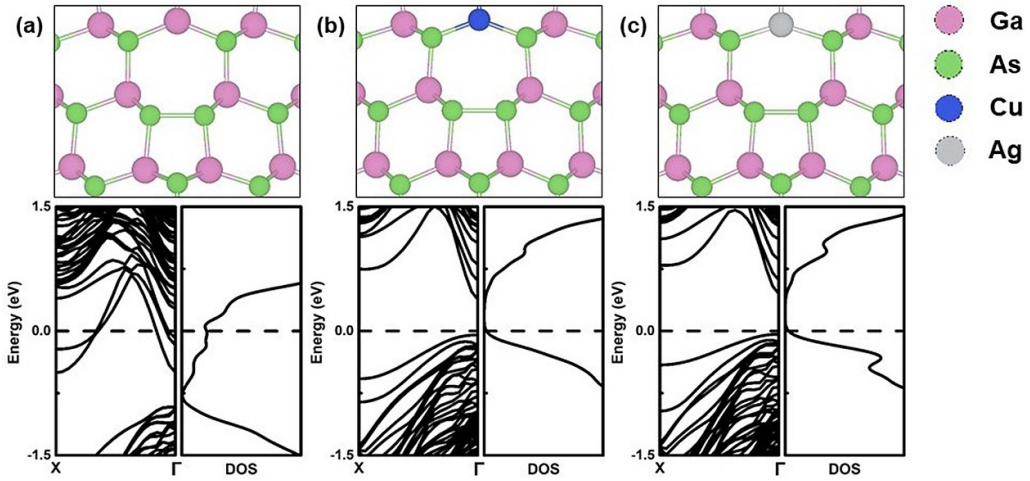

Figure 4. Representative passivation results for GaAs Σ3 (112) As core. (a) Prototype GaAs GB. (b) Cu substitutes Ga3. (c) Ag substitutes Ga3. Cu/Ag substitution subtracts the redundant 2.0 electrons near the GB surface and successfully eliminates the defect states.

We can also apply this analysis process to the CdTe Σ3 Te-core GB (figure 3(b)). According to the LDOS results (figure 2(b)), most of the defect states are contributed by Te-core atoms. We assume that the Te1–Cd4 bond contains approximately 2.0 e and that Te contributes 0.5 e to this bond, as in a normal Te–Cd bond, because of the low degree of bond distortion. In addition, there are two normal Te–Cd bonds located on the Te1 atom. The number of extra electrons near the GB is $2 \times (6 - 3 \times 1.5) = 3.0$.

Based on electron counting, the number of extra electrons at Σ3 anion-core GBs of GaAs and CdTe are two and three, respectively. These numbers provide direct guidance for defect passivation. For example, in CdTe, one can expect six extra electrons in a $1 \times 2 \times 1$ supercell and insert a Cd atom (providing two valence electrons) near the four Te atoms to reach octet saturation. The analysis yield the same passivation method with the operation to dope one Cd atom according to the self-passivation rule for CdTe GBs, which can successfully eliminate the deep levels contributed by the Te core atoms [13]. However, such self-passivation is difficult with the GaAs GB, because four dangling As atoms at the GB interface already form chemical bonds. Therefore, instead of forming new bonds with dangling Te atoms to accept extra electrons, as in a II–VI semiconductor, electrons must be removed from the GB region in a III–V semiconductor. According to the results of electron counting, 2.0 electrons should be removed from the GaAs GB core. Because gaps states are mainly derived from Ga1/Ga2 and Ga3 atoms (figure 3), the Ga3 atom can be substituted with Cu or Ag, each of which has two fewer electrons than Ga. With this substitution, the gap states disappear and a visible gap opens, as shown in figures 4(b) and (c).

3.5. Insights on GB passivation in semiconductor solar cells

The deep levels in GaAs and Si GBs are mainly from abnormal bonds, i.e. from some covalent bonds associate with Ga1/Ga2 or Si3/Si4 (figures 2 (c) and (d)). While those in chalcogenide semiconductor GBs are from dangling bonds located at anion cores (figure 2(b)). The discrepancy in the source of the defect states induces a divergence in post-treatments for different types of zinc-blende semiconductors. As for IV and III–V semiconductor GBs, in order to passivate the defect states, the wrong bond must be broken with a large amount of input strain energy [36]; it is difficult to realize this through interstitial doping. For Si, the hydrogen process was found useful in suppressing the harmful effects of GBs [15, 21]. A theoretical study has shown that hydrogen complexes may break the relatively weak Si–Si bond and passivate the resulting two Si dangling bonds by forming two Si–H bonds [21, 37]. Polycrystalline GaAs solar cell efficiency increases with increases in grain size [16, 38, 39]. This implies that the effects of GBs cannot be ignored and that self-passivation does not occur in GaAs GBs.

However, for chalcogenide semiconductor GBs, dangling bonds are much more easily passivated by doping. The doping atom is likely to provide a more stable quantum state for the electrons in the dangling bonds. Self-passivation is an effective way for CdTe to reach an electrically benign GB structure. The indispensable $CdCl_2$ post-treatment for CdS/CdTe solar cells has been shown to support GB passivation [3, 32]. A density functional theory study proved that Na doping could clearly passivate GB defect states in both CIGS and CZTS [14]. These indicate that chalcogenide semiconductor-based solar cells can achieve high efficiencies without special processes for passivating GBs, or with easily passivated GB defects.

4. Conclusion

In summary, we have systematically studied the electronic structures of typical GBs in zinc-blende semiconductors. We find two distinct GB characteristics in Σ3 (112) zinc-blende GBs: in IV and III–V semiconductors, covalent bonds are formed between pairs of anions, while in II–VI and I–VII semiconductors, no anion–anion bond formation occurs. Such distinct bonding behavior can be attributed to the different

electronegativity of the anion atoms. These two bonding characteristics yield different defect features in these GBs. For the GBs in II–VI and I–VII semiconductors, the defect states can be passivated through the doping of compositional cations or isovalent atoms, while for the GBs in III–V semiconductors, the defect states can only be passivated by removing two electrons, for example, via substituting one Ga atom with a Cu or Ag atom. The present results provide a general picture of the defect states of GBs in zinc-blende semiconductors and a basic understanding of the physics underlying the diverse post-treatment processes developed for different semiconductors. The simple electron counting method is not limited to the mentioned zinc-blende semiconductor GB. The passivation solutions for GBs of other materials can also be designed according to the idea of a targeted doping approach. This work may guide the development of targeted passivation approaches to ameliorate defect states at GBs.

Acknowledgments

We acknowledge the stimulating discussion with Cheng-Yan Liu. X G acknowledges funding support from National Natural Science Foundation of China and Science Challenge Project (TZ2018004). W Y acknowledges funding support from National Natural Science Foundation of China (Grant Nos. 11674237 and 11974257) and the Priority Academic Program Development of Jiangsu Higher Education Institutions (PAPD). Calculations are performed at the Supercomputer Center of Fudan University.

ORCID iD

Xin-Gao Gong https://orcid.org/0000-0001-7539-5471

References

[1] Zook J D 1980 *Appl. Phys. Lett.* **37** 223
[2] Metzger W K and Gloeckler M 2005 *J. Appl. Phys.* **98** 063701
[3] Li C *et al* 2014 *Phys. Rev. Lett.* **112** 156103
[4] Park J-S, Kang J, Yang J-H, Metzger W and Wei S-H 2015 *New J. Phys.* **17** 013027
[5] Yang S, Zhou N, Zheng H, Ong S P and Luo J 2018 *Phys. Rev. Lett.* **120** 085702
[6] Zhu Q, Samanta A, Li B, Rudd R E and Frolov T 2018 *Nat. Commun.* **9** 467
[7] Yan C *et al* 2018 *Nat. Energy* **3** 764
[8] DiStefano T H and Cuomo J J 1977 *Appl. Phys. Lett.* **30** 351
[9] Gloeckler M, Sites J R and Metzger W K 2005 *J. Appl. Phys.* **98** 113704
[10] Kanevce A, Reese M O, Barnes T M, Jensen S A and Metzger W K 2017 *J. Appl. Phys.* **121** 214506
[11] Yan Y *et al* 2015 *J. Appl. Phys.* **117** 112807
[12] Yin W-J, Wu Y, Wei S-H, Noufi R, Al-Jassim M M and Yan Y 2014 *Adv. Energy Mater.* **4** 1300712
[13] Liu C-Y, Zhang -Y-Y, Hou Y-S, Chen S-Y, Xiang H-J and Gong X-G 2016 *Phys. Rev.* B **93** 205426
[14] Liu C-Y, Li Z-M, Gu H-Y, Chen S-Y, Xiang H and Gong X-G 2017 *Adv. Energy Mater.* **7** 1601457
[15] Seager C H and Ginley D S 1979 *Appl. Phys. Lett.* **34** 337
[16] Kazmerski L L and Ireland P J 1980 *J. Vac. Sci. Technol.* **17** 525
[17] Pande K P, Hsu Y S, Borrego J M and Ghandhi S K 1978 *Appl. Phys. Lett.* **33** 717
[18] Ghandhi S K, Borrego J M, Reep D, Hsu Y S and Pande K P 1979 *Appl. Phys. Lett.* **34** 699
[19] Pande K, Reep D, Shastry S, Weiner A, Borrego J and Ghandhi S 1980 *IEEE Trans. Electron Devices* **27** 635
[20] Seager C H and Ginley D S 1981 *J. Appl. Phys.* **52** 1050
[21] Nickel N H, Johnson N M and Jackson W B 1993 *Appl. Phys. Lett.* **62** 3285
[22] Johnson N M, Biegelsen D K and Moyer M D 1982 *Appl. Phys. Lett.* **40** 882
[23] Cho N H, McKernan S, Wagner D K and Carter C B 1988 *J. Phys. Arch.* **49** 245
[24] Yan Y, Al-Jassim M M and Jones K M 2003 *J. Appl. Phys.* **94** 2976
[25] Feng C B, Nie J L, Zu X T, Al-Jassim M M and Yan Y 2009 *J. Appl. Phys.* **106** 113506
[26] Kresse G and Furthmüller J 1996 *Phys. Rev.* B **54** 11169
[27] Blochl P E 1994 *Phys. Rev.* B **50** 17953
[28] Ceperley D M and Alder B J 1980 *Phys. Rev. Lett.* **45** 566
[29] Iarlori S, Galli G, Gygi F, Parrinello M and Tosatti E 1992 *Phys. Rev. Lett.* **69** 2947
[30] Kim Y-H, An S-Y, Lee J-Y, Kim I, Oh K-N, Kim S-U, Park M-J and Lee T-S 1999 *J. Appl. Phys.* **85** 7370
[31] Yan Y, Jiang C S, Noufi R, Wei S H, Moutinho H R and Al-Jassim M M 2007 *Phys. Rev. Lett.* **99** 235504
[32] Zhang L, Da Silva J L F, Li J, Yan Y, Gessert T A and Wei S H 2008 *Phys. Rev. Lett.* **101** 155501
[33] Park J-S 2019 *Phys. Rev. Mater.* **3** 014602
[34] Tong C J and McKenna K P 2019 *J. Phys. Chem.* C **123** 23882
[35] Murat A, Matsubara M, Nguyen B-M and Bellotti E 2018 *Phys. Rev. Mater.* **2** 123604
[36] Zhang L, McMahon W E and Wei S-H 2010 *Appl. Phys. Lett.* **96** 121912
[37] Chang K J and Chadi D J 1989 *Phys. Rev. Lett.* **62** 937
[38] Benner J P and Eugene Blakeslee A 1981 *MRS Proc.* **5** 205
[39] Mohammad S N, Sobhan M A and Qutubuddin S 1989 *Solid State Electron.* **32** 827